Journal of
Theoretical & Computational Science

Bahar, et al., J Theor Comput Sci 2017, 4:1
DOI: 10.4172/2376-130X.1000154

Research Article Open Access

Electrical Properties of Porous Silicon for N_2 Gas Sensor

Mahmood Bahar[1,2*], **Hamideh Eskandari**[2] **and Naghi Shaban**[2]

[1]*Department of Physics, Islamic Azad University, Tehran North Branch, Tehran, Iran*

[2]*Faculty of Physics, Kharazmi University, Tehran, Iran*

[*]**Corresponding author:** Mahmood Bahar, Department of Physics, Islamic Azad University, Tehran North Branch, Tehran, Iran, Tel: +98-21-880-95970; E-mail: bahar@khu.ac.ir

Rec date: May 24, 2017; **Acc date:** June 16, 2017; **Pub date:** June 19, 2017

Abstract

The application of porous silicon (PSi) for gas sensing devices has gained a considerable attention in the last decade. This work considers the electrical features of PSi layers prepared by electrochemical etching. We find that in order to get a better understanding of the absorption properties of PSi surface, it is necessary to know how the PSi morphology depends on the etching parameters. The physical structure of PSi, i.e., porosity, and pore size distribution can be controlled by changing the Hydrofluoric Acid concentration, current density, anodizing length and etching time in anodizing procedure. We describe our test system for gas sensors and investigate on the electrical behavior of PSi layers (p-type) in N_2 gas for various fabrication conditions. The results show that the current density increases significantly as N_2 gas is adsorbed. The measurements of the I-V characteristics were carried out at atmospheric pressure, room temperature, and with N_2 gas as well.

Keywords: Gas sensor; Porous silicon; N_2 gas; Current-voltage curve

Introduction

Today's need to constantly monitor and control the air pollution of the environment, in laboratories, hospitals or generic technical installations pushes the development of highly sensitive gas sensors to prevent accidents caused by gas leakages. Such sensors should allow continuous monitoring of the concentration of particular gases in the environment. Ideally, a gas sensor should have: (i) high sensitivity; (ii) high selectivity, i.e., negligible (or at least a known and repeatable) response to other gases; (iii) small size; and (iv) low cost [1].

Porous silicon (PSi) layers have attracted special attention in chemical sensor applications because of their large internal surface area and an easily modified microstructure. It is found that the electrical or optical characteristics of PSi, e.g., conductivity, capacitance or refractive index may change dramatically upon adsorption of molecules to its surface [2,3]. The Adsorption, e.g., of gas molecules is mainly determined by the physical microstructure of PSi as well as its surface chemical and physical properties.

The physical structure of PSi, i.e., porosity, thickness and pore size distribution can be controlled by changing the hydrofluoric acid concentration, current density, anodization length, porous area and the etching time in the electrochemical etching procedure used to fabricate PSi [4]. On the other hand, the surface chemical properties of PSi can be modified by oxidization, nitridation or other chemical treatments for specific applications [2,4].

In recent years, a lot of efforts have been devoted to introducing new materials into the pores of PSi. Metals, semiconductors and polymers are reported to be partially deposited or to totally fill PSi pores by using the spin coating electrochemical deposition or liquid contact methods [2,5]. Also, because of its very large surface/volume ratio (hundreds of m^2/cm^3), a high reactivity, and its potential compatibility with silicon-based electronics, the (PSi) is one of the most promising materials for the fabrication of gas sensors [6-8].

The PSi-based devices have been proposed as sensors for humidity, gases (like, CF_4, N_2) and various organic polar substances [1]. The involved sensing mechanisms are generally associated with a change in the free carrier concentration in the porous layer due to adsorbed molecules, or changes in the dielectric constant due to gas condensation inside the pores; the sensed quantity is generally a conductance/current or capacitance [1,9].

In these studies, the electrical and optical response of PSi-based sensors has been investigated in the gas medium by performing conductance, capacitance [9-12] and photoluminescence (PL) measurements [13,14]. Both capacitive and ionic sensing modes in PSi are described by Anderson et al. [10], Motohashi et al. [15] expressed gas identification by a single gas sensor using PSi as the sensitive material; Stievenard and Deresmes [3] proposed a simple model based on dangling bonds to explain quantitatively the electrical behavior of Au-porous Si junction in the presence of various gases. Barillaro et al. [16] demonstrated a new integrated sensor with an adsorbing PSi layer that modulates the resistance of a crystalline Si resistor when exposed to organic vapor.

This study is focused on the chemical gas sensing properties of PSi. Si-based chemical gas sensors would be of extreme practical importance; a number of new possibilities are studied such as PL quenching and change in electrical conductivity. The PL quenching of PSi by chemicals has been already suggested for the applications in chemical gas sensors. Nevertheless, sensors based on PL changes are unlikely to be realized due to their highcost. We suggest a different chemical approach, based on the conductivity of PSi rather than the PL quenching. This study is based on our discovery of the tremendous change in the electrical conductivity of PSi when it is exposed to N_2 gas. In the future, this effect could be used as a sensing method for different chemicals in the gas phase. Chemical gas sensors based on electrical conductivity changes in semiconductors are well-known, and

their contribution has been recognized. In this study, we probe the effects of anodization parameters on PSi sensor response. The most appealing features of PSi sensors are their low cost and the simplicity of fabrication [9].

Materials and Methods

The porous silicon layers were prepared from p-type Si, (100) oriented boron-doped (1.4-2.6 Ωcm resistivity) by electrochemical etching in a solution of a HF (40 Wt. %) /ethanol (99.8 Wt. %) /H_2O (by different VOL x/y/z) as an electrolyte, at various current densities, preparation times and anodization lengths [17]. As we know, the mechanism of porous silicon formation in neutral fluoride medium is associated with the two-step mechanism of silicon dissolution [18].

Silicon oxidation: $Si+4H^+ + 2H_2O \rightarrow SiO_2+4H^+$ (S1)

Oxide dissolution: $SiO_2+ 6F+4H^+ \rightarrow SiF^{-2}_6 + 2H_2O$ (S2)

Step (S1) takes place at the bottom of the pores, and the protons generated by this process diffuse through the porous layer, enabling its partial dissolution. A steady-state thickness is obtained when all the protons generated by (S1) are consumed through step (S2) before they can escape from the porous layer. At potentials lower than 20 V, as we did it, the electrochemical current is associated with these two reactions, as indicated by the Koutecky-Levich plots, consistent with a mass transport limitation by diffusion of fluoride species to the electrode [19]. Figure 1 illustrates the experimental set-up used to anodization process and basic reaction of PSi formation. A film of Al was deposited on back of the silicon by high vacuum evaporation, before the formation of the PSi films. The PSi layers grown in this way have pores a few nanometers in diameter.

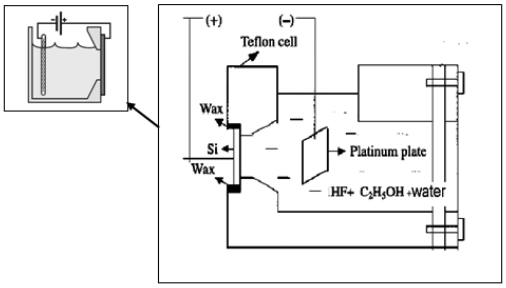

Figure 1: Experimental set up for electrochemical etching.

The experimental parameters for the preparation of the PSi layers tested for this work are collected in Table 1. The PSi layer thicknesses were measured 20-30 μm for the etching time stated and Porosity of the PSi samples was calculated by a gravimetric method.

Psi No.	Current Density (mA/cm^2)	Ratio concentration HF/C_2H_5OH/H_2O	Time (s)	Sample area (cm^2)	Anodization length (cm)	Porosity
1	10	01:03:02	1800	1	4	86%
2	10	01:03:02	1800	1	5	70%
3	10	01:03:02	1800	1	6	61%
4	10	01:02:02	3600	1	4	76%
5	10	02:02:01	1200	1	4	68%
6	10	01:02:01	1200	1	4	45%
7	10	01:02:02	1200	1	4	63%
8	20	01:02:02	1200	1	4	65%

Table 1: Growth parameters of porous silicon layers PSi samples.

After the anodization process, the samples were rinsed with ethanol, and then rinsed twice with distilled water; the water was removed by rinsing with acetone and finally the samples were allowed to dry out in the open. The porous layers were checked for PL under the 435.8 nm line of a Hg Lamp In the next step, a 20-nm layer of gold was deposited on the PSi surface by High vacuum evaporation at room temperature and base pressure on 2×10^{-5} bar to create a semitransparent ohmic electrical contact without filling the pores.

Current was measured using a Keithley 610C electrometer in a two-terminal sandwich configuration: the electrometer provided a stabilized voltage that was applied to each side with the Si wafer. The measured current was in the range of micro to milliamperes. It seems that the inherence of the contact between the gold and the porous silicon is an important topic. To distinguish the contribution to Au-PSi contact and the behavior of PSi, we repeated current measurements of the surface of the PSi with gold. Our results clearly show that the contribution to Au-PSi contact (Schottky junction) is very weak, less than 10-3 Ω, and cannot play major role in the behavior of PSi. In other words, the currents through structure are really determined only by conductivity of PSi. Exposure to chemical gases was carried out in a special box with dimension of $10 \times 10 \times 20$ cm^3. Samples were kept in ambient conditions and were introduced into the box for the chemical exposure measurements. Test gas, containing the desired partial pressure of the chemical gases, was stored in a large and safe container and introduced into the sample chamber by a tube and valve.

Results and Discussion

Structural studies

Figure 2 shows the morphology and pore size of the PSi layer of sample No.1 with 10 mA/cm^2 and 30 minutes anodization time with

different magnification. The surface morphology reveals the nanostructure PSi pores. The bright regions in the figure are the Si structures and the dark regions are the pores. By increasing the porosity of the PSi layers, Si structures decrease while the size of the pores increases.

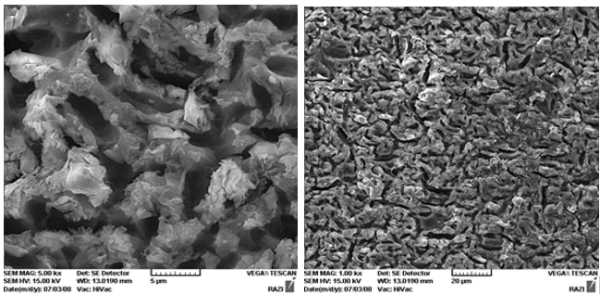

Figure 2: FESEM images of PSi sample prepared at 10 mA/cm^2 for 1800 s in l: 3: 2 HF/ C_2H_5OH / H_2O solution and 4 cm iodization length.

Photoluminescence (PL) properties

The PL emission peaks of samples were measured at room temperature. Figure 3a shows typical PL curves of the samples obtained at current density of 10 mA/cm^2, and different etching times. The peaks show a blue shift with increasing the etching time and porosity. The band gap energy versus porosity is shown in Figure 3b. In this study, the band gap increased from 1.780 to 1.828 eV by increasing the porosity. The band gap value increased with increasing the porosity due to change in the Si structure size [20,21]. The PSi energy gap is definitely having higher energy gaps compared to Silicon (1.11eV). The extracted values of band gap are in the same range of the reported results (1.5-2.5 eV) for PSi samples [22-24].

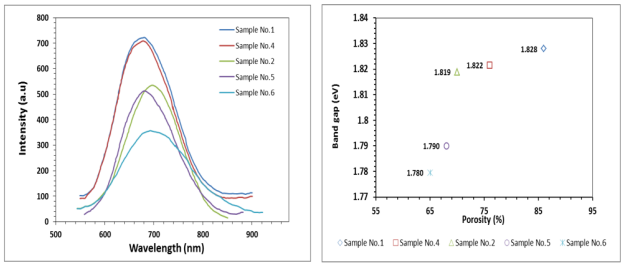

(a) (b)

Figure 3: (a) PL peaks for PSi samples prepared under a fixed current density (J=10 mA/cm^2) and different etching time, (b) Band gap vs. porosity extracted from PL spectroscopy for PSi samples.

Electrical properties (current-voltage characteristics)

The current-voltage behavior of our device in the presence of air at room temperature and ambient pressure is not symmetrical with respect to zero voltage. Figure 4 presents a schematic cross section of a device with electrical contacts. We observe a small response current from the sensor for negative bias, due to rectifying behavior of the PSi junction. For this reason, all measurements were performed at forward polarization (positive bias on top gold contact relative to aluminum backside contact). This result is in good agreement with the results of Stievenard et al. [3].

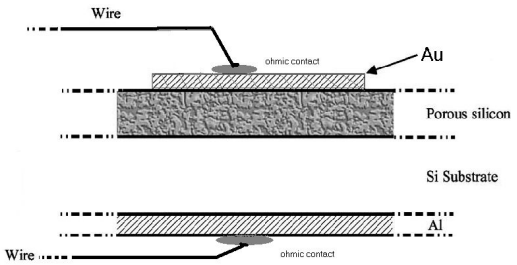

Figure 4: Cross-section of Au/ PSi / Al sandwich device with electrical contacts.

Concentration effect: With an increasing concentration of HF, ethanol and H_2O, the porosity in the PSi sample increases and then more N_2 molecules can be adsorbed on PSi surface, increasing the conductivity. In Figure 5, the concentration of acid, ethanol and H_2O is different for each sample (samples No.5, 6 and 7). It can be seen from Figure 5 that increasing the concentration of acid, ethanol and H_2O in electrolyte solution increases the porosity in PSi samples. Therefore, more N_2 molecules can be adsorbed in PSi surfaces, and as a result conductivity increases parameters were the same Table 1.

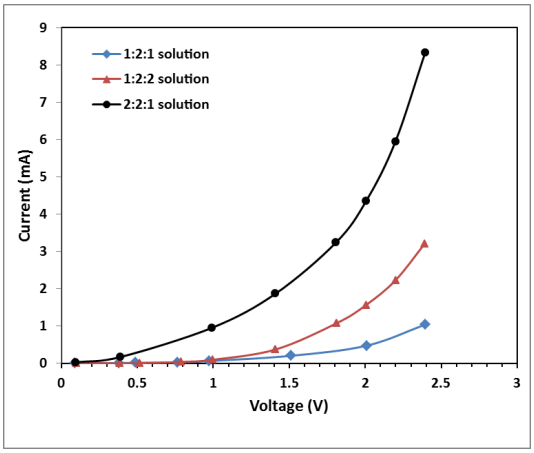

Figure 5: Effect of catalyst concentration on the current-voltage behavior in N_2 gas (320 Pa) of 1.0 cm^2 porous Si samples prepared at 10 mA/cm^2 for 1200 s, 1:2:1, 1:2:2 and 2:2:1 HF/ C_2H_5OH /H_2O solution and 4 cm anodization length.

The effect of anodization length: To show the effect of anodization length, in Figure 6, three samples are compared. As we can see from Table 1, anodization length of sample No. 3 is larger than the samples No. 2 and 1, while the other fabrication parameters are kept the same. One can predict that a decrease of the Anodization Length (A. L.) will allow more N_2 molecules to be adsorbed into the PSi samples, resulting in the increase in current seen in Figure 6. Actually, there is a balance between the decreases of anodization length with greater porosity, so more current can flow through nanowires in the PSi layer.

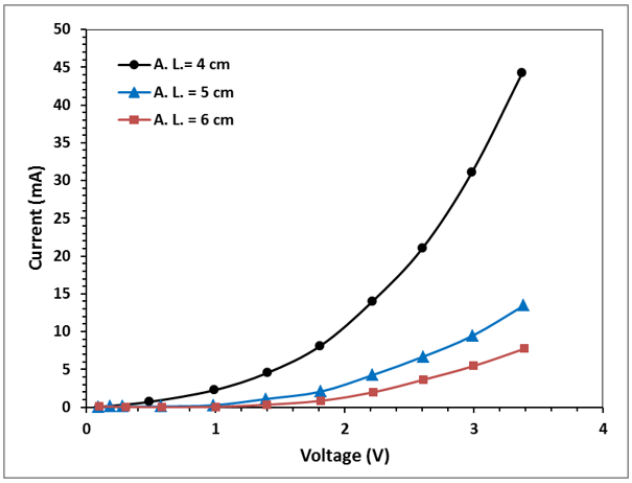

Figure 6: The Effect of anodization length (A. L.) of samples on the current-voltage response to N_2 gas (320 Pa) of porous Si Samples prepared at 10 mA/cm^2 for 1800 s in l: 3: 2 HF/ C_2H_5OH / H_2O solutions and 6, 5 and 4 cm anodization length.

Etching time effect: Figure 7 illustrates the results obtained from current-voltage measurements of different etching time. The effects of two samples are compared. As we see, the etching time of sample No. 4 is three times longer than the etching time of sample No. 7, while the other situations of electrochemical etching process are kept constant in both two samples. Figure 7 represents significantly increase of porosity in our samples due to increase of the etching time, so more N_2 gas molecules can be captured in PSi surface. For this reason, we can see an increase in electrical conductivity of PSi.

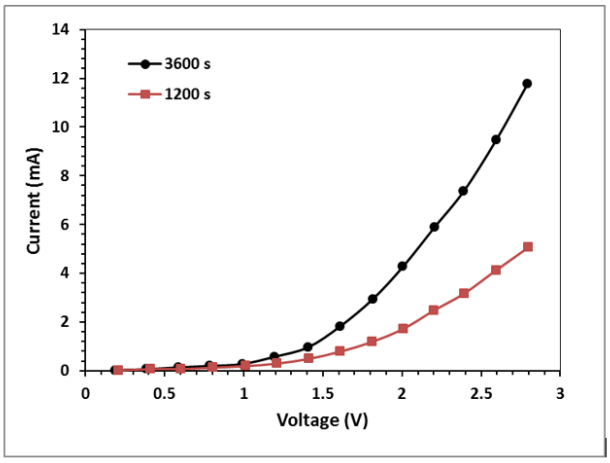

Figure 7: Effect of electrochemical etching time on the current-voltage behavior of porous Si Samples prepared at 10 mA/cm^2 in l: 2: 2 HF/ C_2H_5OH / H_2O solution : 4 cm anodization length.

Gas exposure and measurements: The current voltage (I-V) characteristics of Au/Psi/Al structure, shown in Figure 8, were measured in the air environment and N_2 gas environment, in order to evaluate the response and sensitivity of the devices. The current response of the devices shows generally that for values of applied bias less than 1 V, an ideality factor of 1.12 is determined, which suggests a Schottky-like junction. After we introduced N_2 gas, a continuous increase in the conductivity was observed for the entire applied voltage range. For example, this increase at 3.5 V forward bias is about a factor of 5 mA. rectifying behavior is also observed when the gas is introduced into the chamber with no change in the shape of I-V curve, only a change in current magnitude at fixed voltage.

For comparison, in Figure 8, the current-voltage behavior of sample No. 6 and a pristine Si wafer in N_2 medium is shown. A rectifying behavior is seen for Si in Figure 8. The behavior is coming mainly from Schottky junction between gold and silicon. However, a large increase in the conductivity was observed for the etched PSi sample as there are pores to be filled by N_2 gas. The increase in 3.6 V forward bias is a factor of 4. This figure shows that PSi samples are much more sensitive to gas than a Si wafer.

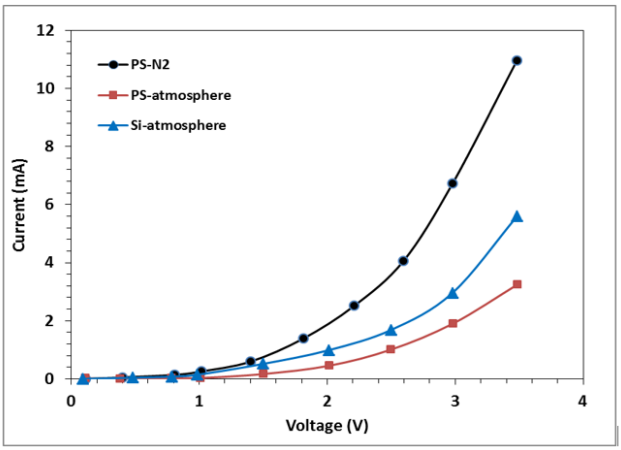

Figure 8: Current-voltage comparison behavior in air and in pure N_2 of 1 cm^2 porous Si sample prepared in 1:2:1 HF/ C_2H_5OH / H_2O solutions at a current density of 10 mA/cm^2 for 1200 s and Si wafer.

The exposure of the structure to N_2 gas did not change the shape of the characterize current-voltage dependence but only changes the current magnitude at the fixed voltage. When the gas is removed, the current recovers rapidly and completely to the initial value. A Nano exponential decrease of the current is observed [25]. There are several approaches to explain the variation of the current. The most popular is associated with the condensation of gas in the pores. Anderson et al. claim that this condensation changes the dielectric constant in the pore. However, Schechter et al. [26] showed by measuring the refractive index of PSi layer that there was no condensed liquid when the change in conductivity began. Thus, we propose that the conductivity is governed by the density of charges trapped on the interface states.

The effect of the gas is to passivate the active dangling bond, perhaps through a screening mechanism, so that the depleted thickness decreases and the width of the channel increase. It appears that a depleted region develops between the PSi layer and Si substrate during electrochemical anodization. The reason for the development of this region is the movement of electrons from the PSi layer to the Si substrate and recombination with positive charges. As a result, in the

PSi layer, positive space charge will exist and, in the Si substrate, negative space charges.

At this stage, some of the important issues are to obtain a depleted region and its effect on dangling bonds for our samples. It is known from the electron paramagnetic resonance measurements that a typical surface concentration of dangling bonds is around 109 cm^{-2}. The developed surface of our layer is on the order of 200 m^2/cm^3. Since the initial doping density of the Si is of the order of 6×10^{15} cm^{-2}, there is enough density of dangling bonds to passivate the free carriers (only a few percent of the density of dangling bonds are necessary) [9]. The integration of Poisson's equation leads to a simple relation between depleted region (W) and density (σ), given by:

$$W=\sigma/N_A$$

where N_A is the doping level of the Si in our samples, column diameters are on the order of 10 nm [27]. Using Equation (1), we find that W is on the order of a few nanometers, i.e., in the range of half of the column diameter. So, the density of dangling bonds is high enough to passivate the free carriers and consequently the channel could be pinched easily, severely restricting conduction.

A second test consisted of measuring the device's resistance as a function of time using polarization voltage. Initially the chamber was evacuated down to 2 mbar; once that pressure was obtained N_2 gas was injected until reaching around the atmospheric pressure and then the value of the resistance was measured in the times. Figure 9 presents the electric responses of sample No. 8 at atmospheric pressure, at 2 mbar and in N_2 atmosphere. Additionally, it shows the 20 and 40 min curves after N_2 were injected. The behavior of the sample at atmospheric pressure is very similar to its behavior at the indicated vacuum, indicating that the air contained in the sample does not affect its electric behavior. A current increment for positive voltages is observed when N_2 gas is injected; this current keep rising as the contact time between sample and N_2 gas increases. The current increased approximately one order of magnitude for 40 min after N_2 gas injection, compared to its value for the sample in vacuum.

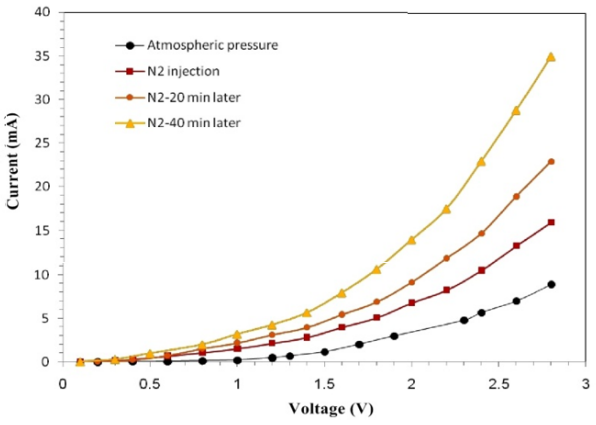

Figure 9: Effect of time duration in presence of N_2 gas, (20 min- 40 min) for porous Si sample prepared in 1:2:1 HF/ C_2H_5OH / H_2O solutions at a current density of 20 mA/cm^2 for 1200 s.

N_2 gas Molecules passivated the PSi structure by reducing on the material's skeleton surface the great density of imperfections acting as traps for the circulating electrons. The response to the N_2 gas is more noticeable as exposure time increases since PSi structure is very complex, packed with imperfections and tunnels such that N_2 gas takes a long time to reach deep inner locations. The response to N_2 gas for samples prepared at anodization currents greater than 10 mA/ cm^2 (high porosity) was low, possibly because of a slide on the PSi skeleton due to high tensions suffered by the material in the drying process. The resistivity change of the PSi film is low in this case, which makes very difficult to detect any change of it when the sample is in contact with the gas [28].

To avoid complications in the mechanism of conductivity [26] the enhancement of the conductivity has been considered by two phenomena. The first-one is that there are no chemical reactions between PSi surface states and gas molecules. The enhancement of conductivity is a physical mechanism due to an extra current through the adsorbed molecules, in addition to the current through the Si skeleton. This mechanism includes the dipole moment of the adsorbed species, promoting an enhancement of the total current through the porous layer. The latter [9] is the chemical reactions between dangling bonds and adsorbed molecules occur inside pores, due to the adsorbed species, when they are oxidized; therefore, there is an improved passivation of dangling bonds, which enhances the conductivity [29]. And in turn change the behavior of PSi gas sensors, such as the sensitivity, etc. The knowledge of the dependence on the anodization parameters could allow one to design a PSi with predicted properties to serve for the intended applications.

Conclusion

We have studied the behavior of our PSi samples under various conditions. The porosities of our PSi samples were properly characterized and consistent with the etching conditions. In this study, we clearly identified an increase in conductivity of PSi samples by increasing of some anodic parameters such as etching time, electrolyte concentration, etc. and a decrease for increasing of some other parameters of electrochemical etching like anodizing length. These results are due to an obvious modification of band gap magnitude after the etching process. These also showed that greater porosity gives greater conductivity in expose of N_2 gas. We have prepared a set of PSi samples, fabricated with different anodization parameters (i.e., current density, ratio concentration, sample area, etc.), and we have conducted current measurements as a function of applied voltages on the PSi. By changing the anodization parameters, it is possible to modify the morphological properties of PSi layers (i.e., porosity, surface/volume ratio, etc.). For each condition, a non-linear current enhancement was observed as a function of applied voltage. This means that the chemical nature of the adsorbents have a considerable influence on the conductivity, which is favorable for sensor applications. Also, we observed Non-significant decrease in conductivity of our samples after anodization in absence of gas molecules. This could be justified by this assumption that after anodization we have some crystallite spherical boundary as the surface of our samples which cause of increase in band gap and also decrease in conductivity. We can notice that the increase in conductivity due to the increase in time duration that N_2 gas was passed through our chamber.

References

1. Barillaro G, Nannini A, Pieri F (2003) APSFET: A new, porous silicon-based gas sensing device. Sensors and Actuators B: Chemical 93: 263-270.

2. Wang G, Arwin H (2002) Modification of vapor sensitivity in ellipsometric gas sensing by copper deposition in porous silicon. Sensors and Actuators B: Chemical 85: 95-103.
3. Stievenard D, Deresmes D (1995) Are electrical properties of an aluminum–porous silicon junction governed by dangling bonds? Applied Physics Letters 67: 1570-1572.
4. Herino R, Bomchil G, Barla K, Bertrand C, Ginoux JL (1987) Porosity and pore size distributions of porous silicon layers. Journal of the Electrochemical Society 134: 1994-2000.
5. Moreno JD, Marcos ML, Agulló-Rueda F, Guerrero-Lemus R, Martı́ RJ, et al. (1999) A galvanostatic study of the electrodeposition of polypyrrole into porous silicon. Thin Solid Films 348: 152-156.
6. Bahar M, Dermani EK (2017) Structural, electrical and optical properties of TiO2 thin film deposited on the Nano porous silicon template. Surface Review and Letters 1850017.
7. Bahar M, Gholami M, Azim-Araghi ME (2014) Sol–gel synthesized Titania nanoparticles deposited on porous polycrystalline silicon. Improved carbon dioxide sensor properties. Materials Science in Semiconductor Processing 26: 491-500.
8. Çomakli O, Yazici M, Yetim T, Yetim AF, Çelik A (2016) Tribological properties of TiO2/SiO2 double layer coatings deposited on CP-Ti. Surface Review and Letters 1750082.
9. Khoshnevis S, Dariani RS, Azim-Araghi ME, Bayindir Z, Robbie K (2006) Observation of oxygen gas effect on porous silicon-based sensors. Thin Solid Films 515: 2650-2654.
10. Erson RC, Muller RS, Tobias CW (1990) Investigations of porous silicon for vapor sensing. Sensors and Actuators A: Physical 23: 835-839.
11. Kim SJ, Lee SH, Lee CJ (2001) Organic vapour sensing by current response of porous silicon layer. Journal of Physics D: Applied Physics 34: 3505.
12. Fürjes P, Kovács A, Dücso C, Ádám M, Müller B, et al. (2003) Porous silicon-based humidity sensor with interdigital electrodes and internal heaters. Sensors and Actuators B: Chemical 95: 140-144.
13. Letant SE, Tan TT, Zenhausern F, Sailor MJ (2000) Integration of porous silicon chips in an electronic artificial nose. Sensors and Actuators B: Chemical 69: 193-198.
14. Holec T, Chvojka T, Jelınek I, Jindřich J, Němec I, et al. (2002) Determination of sensoric parameters of porous silicon in sensing of organic vapors. Materials Science and Engineering: C 19: 251-254.
15. Motohashi A, Kawakami M, Aoyagi H, Kinoshita A, Satou A (1995) Gas identification by a single gas sensor using porous silicon as the sensitive material. Japanese Journal of Applied Physics 34: 5840.
16. Barillaro G, Nannini A, Pieri F, Strambini LM (2004) Temperature behavior of the APSFET—a porous silicon-based FET gas sensor. Sensors and Actuators B: Chemical 100: 185-189.
17. Gabouze N, Belhousse S, Cheraga H, Ghellai N, Ouadah Y, et al. (2006) CO_2 and H_2 detection with a CHx/porous silicon-based sensor. Vacuum 80: 986-989.
18. Chazalviel JN, Ozanam F (2011) Electrochemically formed porous silica. Materials 4: 825-844.
19. Parkhutik V (1999) Porous silicon—mechanisms of growth and applications. Solid-State Electronics 43: 1121-1141.
20. Behzad K, Yunus WMM, Talib ZA, Zakaria A, Bahrami A (2012) Effect of preparation parameters on physical, thermal and optical properties of n-type porous silicon. Int. J. Electrochem. Sci 7: 8266-8275.
21. Ee DTJ, Sheng CK, Isa MIN (2011) Photoluminescence of porous silicon prepared by chemical etching method. Malaysian Journal of Analytical Sciences 15: 227-231.
22. Rajabim M, Dariani RS (2009) Current improvement of porous silicon photovoltaic devices by using double layer porous silicon structure: applicable in porous silicon solar cells. Journal of Porous Materials 16: 513-519.
23. Sheng CK, Yunus WMM, Yunus WMZW, Talib ZA, Kassim A (2008) Characterization of thermal, optical and carrier transport properties of porous silicon using the photoacoustic technique. Physica B: Condensed Matter 403: 2634-2638.
24. Srinivasan R, Jayachandran M, Ramachandran K (2007) Photoacoustic studies on optical and thermal properties of p-type and n-type nanostructured porous silicon for (100) and (111) orientations. Crystal Research and Technology 42: 266-274.
25. Cheraga H, Belhousse S, Gabouze N (2004) Characterization of a new sensing device based on hydrocarbon groups (CHx) coated porous silicon. Applied Surface Science 238: 495-500.
26. Schechter I, Ben-Chorin M, Kux A (1995) Gas sensing properties of porous silicon. Analytical Chemistry 67: 3727-3732.
27. Sabet-Dariani R, Haneman D (1994) Heat-treatment effects on porous silicon. Journal of Applied Physics 76: 1346-1348.
28. Martinez HM, Rincon NE, Torres J, Alfonso JE (2008) Porous silicon thin film as CO sensor. Microelectronics Journal 39: 1354-1355.
29. Smith RL, Collins SD (1992) Porous silicon formation mechanisms. Journal of Applied Physics 71: R1-R22.